C. R. Physique 15 (2014) 119–125

Contents lists available at ScienceDirect

Comptes Rendus Physique

www.sciencedirect.com

Electron microscopy / Microscopie électronique

Measuring three-dimensional positions of atoms to the highest accuracy with electrons

Utiliser un faisceau d'électrons pour mesurer dans l'espace tridimensionnel la position des atomes avec la plus grande précision

Christoph T. Koch *, Wouter Van den Broek

Institute for Experimental Physics, Ulm University, 89081 Ulm, Germany

ARTICLE INFO

Article history:
Available online 20 January 2014

Keywords:
Inverse dynamical electron scattering
Compressed sensing
Atomic resolution tomography
Low-voltage electrons

Mots-clés :
Inversion directe de diffusion multiple des électrons
Acquisition comprimée
Détermination des structures atomiques en trois dimensions

ABSTRACT

Recent developments in transmission electron microscopy (TEM) have pushed lateral spatial resolution to well below 1 Å. For selected perfect crystal structures, this allows atomic columns to be identified along several crystallographic orientations. Measuring the three-dimensional position of every atom within a TEM specimen, called by some the holy grail of electron microscopy, seems therefore within reach. In this paper, we will discuss recent approaches to this problem and present our own dose-efficient approach that is based on the direct inversion of multiple electron scattering within the sample and that can be applied to various coherent detection schemes, such as high-resolution TEM, confocal scanning TEM, or ptychography. One particular advantage of this approach is that data for only a very limited range of specimen tilt angles is required, and that it can handle the highly dynamical scattering associated with lower electron beam energy.

© 2013 Académie des sciences. Published by Elsevier Masson SAS. All rights reserved.

RÉSUMÉ

Les progrès récents de la microscopie électronique à transmission (TEM) ont poussé la limite de résolution spatiale dans le plan de l'échantillon bien au-delà de 1 Å. Pour des structures cristallines parfaites, ceci permet de visualiser las colonnes atomiques selon plusieurs directions cristallographiques. Mesurer la position tridimensionnelle de chaque atome au sein d'un échantillon TEM, ce qui a parfois été considéré comme le saint Graal de la microscopie électronique, semble désormais accessible. Dans cette contribution, nous introduisons les approches récentes visant à atteindre cet objectif et présentons la nôtre, qui est particulièrement efficace en termes de dose requise. Elle repose sur une inversion directe des mécanismes de diffusion multiple au sein de l'échantillon et peut être adaptée à différents types de détection : TEM haute résolution, STEM confocal et ptychographie. Un de ses avantages spécifiques est de ne requérir qu'un nombre limité de projections. Un autre est de s'adapter très bien aux processus de diffusion multiple subis par des faisceaux incidents de plus faible énergie.

© 2013 Académie des sciences. Published by Elsevier Masson SAS. All rights reserved.

* Corresponding author.

1631-0705/$ – see front matter © 2013 Académie des sciences. Published by Elsevier Masson SAS. All rights reserved.
http://dx.doi.org/10.1016/j.crhy.2013.10.004

1. Introduction

Elastic scattering of electrons is a very sensitive probe for the local arrangement of atoms for two reasons: Firstly, the 10^4–10^5-times stronger interaction of a beam of fast electrons with matter than, for example X-rays [1], makes it possible to measure elastic electron diffraction from individual atoms, without making use of fluorescence. High-resolution transmission electron microscope (HRTEM) images and high-resolution scanning transmission electron microscope (STEM) images of individual atoms kept in place by some sturdy support have been captured [2–6], and nanocrystals only a few cubic nanometers big are sufficient to produce single-crystal diffraction patterns. Secondly, modern electron optics, namely the development of aberration correctors [7,8] and the improvement of instrument stability allow electron beams to be focused to probes as small as 0.5 Å in diameter, and images, featuring an equally good spatial resolution, to be formed [9].

When speaking about the accuracy with which atom positions can be measured, it must be clear that we are always talking about the equilibrium position about which the atom may oscillate more or less strongly, depending on the temperature of the specimen (including local heating by the electron beam) and how tightly the atom is bound to its environment. Single-crystal diffraction measurements can determine such equilibrium positions very accurately, because equivalent atom sites in the whole crystal are being averaged over. However, when measuring the position of an individual atom, the electron dose required to perform this measurement becomes a very important parameter. Most biological materials cannot be imaged at atomic resolution due to the severe structural changes introduced by the probing electron beam [10], so measurements of the positions of individual atoms must be restricted to those (inorganic) materials that are more resistant to electron beam irradiation damage.

In the context of atomic-resolution imaging, the distinction between resolution and accuracy is very important. If we have an instrument capable of imaging the three-dimensional equilibrium positions of individual atoms,[1] its resolution only needs to be about 2 Å in all three dimensions, since two atoms will never be closer to one another than the sum of their ionic radii. The precision with which the three-dimensional center of mass of the image of the atom can then be determined depends largely on the signal quality and thus on the invested electron dose [12,13], a topic that will not be discussed in depth here. The accuracy with which we can determine atom positions depends then, in addition to the signal quality, also on the validity of the mathematical model that links the configuration of atoms to the image intensity. Due to the very high scattering cross section of electrons in matter, one very important criterion for the quality of this mathematical model is the accuracy with which multiple (also called dynamical) scattering is treated.

2. Possible paths towards measuring 3D atom positions

Due to the small scattering angles of at most 50 mrad which can currently be transferred by high-end electron optics for both probe- and image-forming aberration-corrected electron lenses, the longitudinal resolution, along the z-direction, i.e. along the direction of propagation of the electron beam, is generally much worse than the lateral resolution. While the lateral resolution in both STEM and TEM experiments has already been demonstrated to be below 0.5 Å, even sophisticated experimental setups, such as scanning confocal electron microscopy (SCEM) in an aberration-corrected STEM can at best resolve 3 nm along the z-direction [14]. However, although a very special case and not the actual subject of our discussion here, an individual atom may be located with a precision of as low as 0.5 nm in the direction parallel to the trajectory of the electron beam, even if the depth of focus, i.e. the actual resolution along that direction, is only 7 nm [15]. If some prior knowledge of the atomic species present in the sample is already available, then model-based reconstruction methods may be employed which, given sufficiently good signal-to-noise properties, may help to achieve true atomic resolution 3D reconstructions from HAADF–STEM depth-sectioning data [16].

An obvious solution to obtain equally good resolution in all three dimensions seems to be tomography, which allows the reconstruction of a three-dimensional object from projections along many different directions. This approach has recently indeed been shown to yield a 3D atomic resolution reconstruction of metallic nanoparticles [13,17,18]. However, for standard, slab-like sample geometries, it is not generally possible to tilt the specimen by very large angles and still maintain atomic resolution. Also, tomographic reconstruction algorithms require the data to be linear projections, or at least monotonic in the product of local density and thickness. While, for moderate specimen thicknesses, HAADF–STEM approximates this behavior fairly well [19,20], HRTEM image contrast is highly non-linear, since for thin specimens the structural information is mostly reflected in the phase of the transmitted electron wave function, and only affects the image intensity due to spatial-frequency-dependent phase shifts experienced by the electron wave function when passing through the imaging optics (mainly the objective lens, the stigmator and/or the aberration corrector) of the TEM. This close-to-linear behavior of the phase shift of thin objects can be recovered when employing methods capable of (indirectly) measuring relative phase shifts within the electron wave function, such as off-axis electron holography [21,22] and inline holography (also called focal series reconstruction) [23–31]. While off-axis holography is more efficient in reconstructing low-frequency details of the phase of the scattered electron wave, phase maps reconstructed from inline holography seem to suffer less noise per dose at high spatial frequencies [32], and we expect information about the 3D position of atoms to be mostly contained in the high-angle scattering.

[1] Note that atom probe tomography (see [11] for a recent review) does not fall into this category, because it always extracts atoms from the surface of the sample.

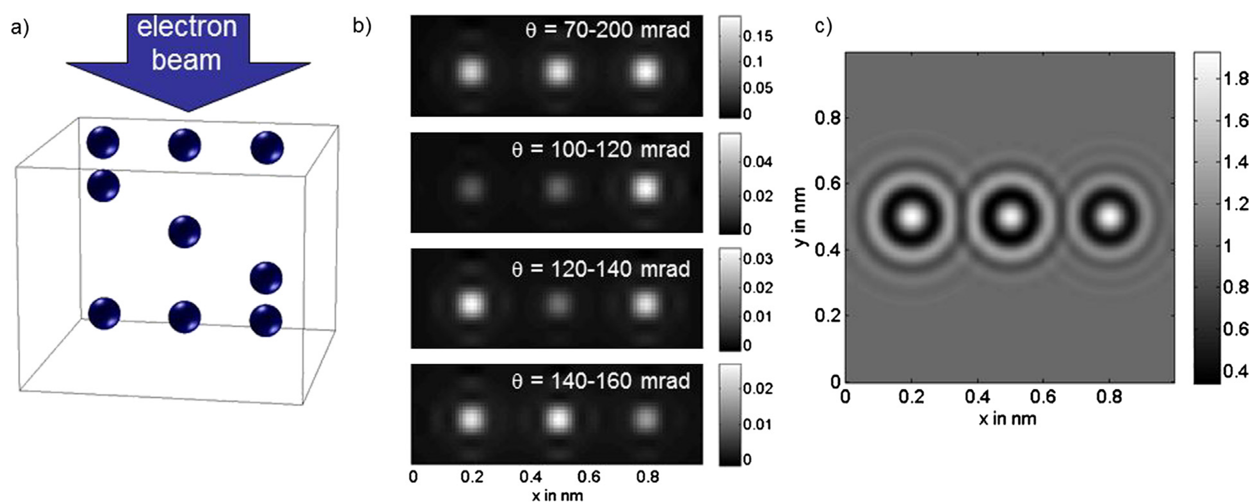

Fig. 1. (Color online.) a) Test structure comprising three atomic columns consisting of three atoms each. b) Simulated 60-kV–HAADF–STEM images for four different detector configurations of the structure shown in a) (semi-convergence angle of the probe $\alpha = 40$ mrad, spherical aberration $C_s = 0$, and defocus $C_1 = 0$). TDS was included by averaging over 80 different configurations. c) Simulated 60-kV–HRTEM image of the same structure (illumination semi-convergence angle $\alpha = 0.1$ mrad, $C_s = 0$, $C_1 = 2$ nm, focal spread $\Delta f = 0.5$ nm). The gray scales indicate the fraction of detected electrons, i.e. the incident flux is 1 electron per pixel. The simulations have been carried out using the qstem software package [41].

In principle, it is also possible to obtain the phase of the scattered electron wave function in reciprocal space, i.e. from electron diffraction measurements. While coherent diffractive imaging (CDI—see [33,34] for recent reviews) uses additional information about the object, such as the knowledge that it is compact, or sparse in some basis, ptychography [35,36] uses multiple diffraction patterns from overlapping areas on the specimen. However, at very high spatial resolution, diffraction-based measurements are limited by the thermal vibration of the atoms. While thermal diffuse scattering (TDS) seems to produce a rather smooth background in HRTEM imaging (but even that is not perfectly clear yet, see [37]), it is highly structured in reciprocal space at diffraction angles corresponding to a spatial resolution of about 1 Å and higher, and thus overlaps with the fine (and often quite weak) interference signal that diffraction imaging techniques depend on [38].

Going into the details of how different TEM imaging or diffraction techniques are limited by experimental conditions in how well they can reconstruct various details of an arrangement of atoms is beyond the scope of this paper. Here, we want to address how, in principle, the reconstruction of 3D atom positions may be implemented in an efficient way, putting as little constraint as possible on the range of samples that can be examined. In particular, we are looking for a technique that allows the investigation of conventional, slab-shaped objects, and is not limited to nanoparticles. Conventional tomographic reconstruction algorithms, for comparison, rely on the availability of linear, or at least monotonic projections of the structure being investigated. In order to minimize the so-called missing-wedge artifacts, the range of tilt angles should be rather large, typically of the order of 140°, i.e. ±70°. For slab-shaped specimen geometries, the problem with such high tilt angles is self-shadowing, i.e. at large tilt angles the projected specimen thickness increases rather quickly, since it varies with the inverse cosine of the tilt-angle.

Fig. 1 shows three simulated ADF–STEM images, as well as an HRTEM image simulated for an artificial arrangement of Au atoms. The three atom columns in this example only differ in the vertical position of the central atom. Due to the low accelerating voltage of only 60 kV, the scattering at high angles is quite strong, and it becomes obvious that both HRTEM and the STEM signal are, in principle, sensitive to the z-position of the central atom, if the signal is analyzed as a function of the scattering angle. Noise has not been included in these simulations, but the small fraction of electrons being detected on the thin, 20-mrad-wide annular detectors corresponding to the lower 3 HAADF–STEM images of $\leqslant$5% of the incident electron flux indicates that, for comparable doses, the HRTEM image might be less noisy, since the contrast is almost comparable. Another difference in the simulation is that accurate HAADF–STEM image simulations require the use of the frozen phonon approximation [39] and are thus very time consuming, whereas the effect of atomic vibrations on the HRTEM image contrast is negligible [40].

While there may potentially be differences in the efficiency with which various acquisition methods transfer this information, Fig. 1 indicates that it should be possible to extract 3D atom positions without having to acquire a large angular range tomographic tilt series with the z-resolution of the linear reconstruction defined by the so-called 'missing wedge'. In fact, by assuming the weak phase approximation, which does not take into account multiple scattering, and also neglecting the interference of waves scattered by neighboring atoms, Van Dyck et al. [42] have shown that the z-position of the bottom atom in 1-layer and 2-layer graphene can be reconstructed with quite high spatial resolution. Since this approach cannot resolve eclipsing atoms, it cannot be considered a full 3D reconstruction, but at least it shows that atomic resolution information in the z-direction can be retrieved from a single projection, if we assume to be able to detect the scattering of

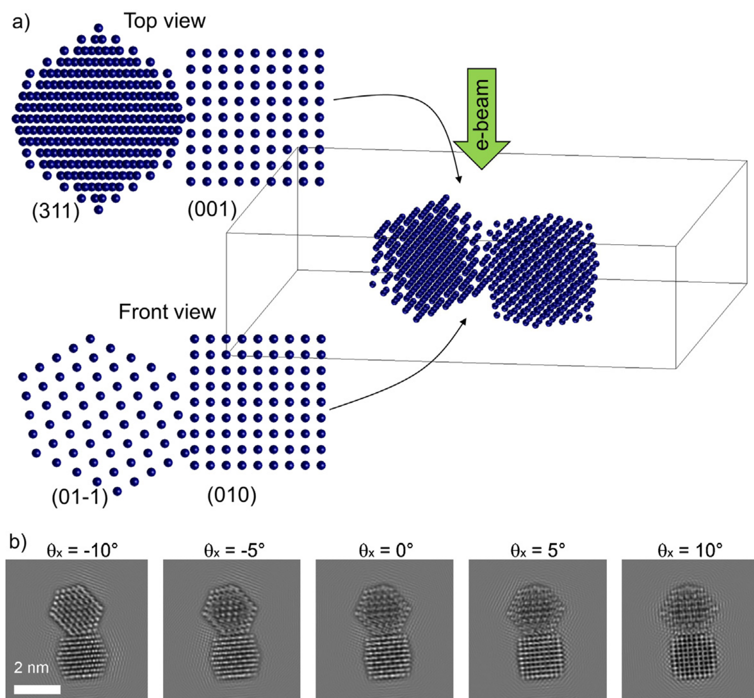

Fig. 2. (Color online.) a) Model of 2 cuboctahedra in different orientations (left particle: (311) zone axis, right particle: (001) zone). In projection the atoms of the left particle are very densely spaced. b) Example HRTEM images simulated for the model shown in a) for 5 different specimen tilts about the horizontal x-axis ($\theta_y = 0°$). The images have been simulated for 40-keV electrons, a spherical aberration of 14 μm, and a focus value of 10.15 nm. A realistic modulation transfer function (MTF) parameterized according to [47] has been applied. A magnification corresponding to a CCD pixel size of 0.25 Å has been assumed.

each atom independently and neglect multiple scattering or interference. The information content of HRTEM images with regard to 3D specimen information has also been discussed in a more general, model-based context [43].

3. Retrieving 3D atom positions from HRTEM images or diffraction patterns

For thicker specimens, especially at low accelerating voltages, the weak-phase object approximation is far from valid, and multiple scattering must be taken into account. Including multiple scattering, partial spatial and temporal coherence, as well as a realistic detector point spread function. We have recently shown that the highly non-linear system of equations, describing the dynamical scattering of electrons, can be inverted by casting it into the form of an artificial neural network and applying the well-established back-propagation algorithm for such systems for very efficient computation of gradients. Applying this principle, and, in some cases, combining it with the charge-flipping algorithm [44] we have developed an iterative reconstruction algorithm capable of recovering the three-dimensional potential distribution of the scattering object from a series of images acquired for a small range of different relative tilt angles between the specimen and the incident electron beam [45]. More recently, we have shown that this reconstruction algorithm should also work with data acquired in a ptychography or SCEM experiment, and that, along with the reconstruction of the object, also some of the experimental parameters can be refined from inaccurate initial estimates [46].

Because the electrostatic potential within a material is simply the sum of potential contributions from each of the atoms within it, the reconstructed potential distribution, deconvolved by the potential of a single atom features sharp peaks at places where the atoms are located [19]. Since each atom occupies some atomic volume, we only expect a single such peak per atomic volume. Silicon, for example, has a density at room temperature of $\rho = 2.33$ g/cm^3 and an atomic weight of $M = 28.1$ g/mol. We thus expect the reconstructed object potential to have a peak density of 1 peak per atomic volume $V_a = M/(\rho N_A) = 20$ Å^3. Sampling the three-dimensional space containing the scattering object with discrete voxels, only a few of these voxels would thus be non-zero, i.e. this discretized potential volume would be quite sparse. For a voxel size of $0.2 \times 0.2 \times 2$ Å^3 only one out of 250 such voxels would be non-zero. For materials containing different atomic species, a generalized atomic potential representing an average of the electron scattering factors of the species present in the material would be used.

Such sparsity is an essential element in the mathematical framework of compressed sensing (CS) [48,49]. CS theory states that a unique solution for an underdetermined system of equations can be found if this solution is sufficiently sparse in some object-basis, and the basis in which the measurement is performed is sufficiently incoherent with the object basis [50]. We have just illustrated that, at sufficiently high spatial sampling, the electrostatic potential of any arrangement of atoms is

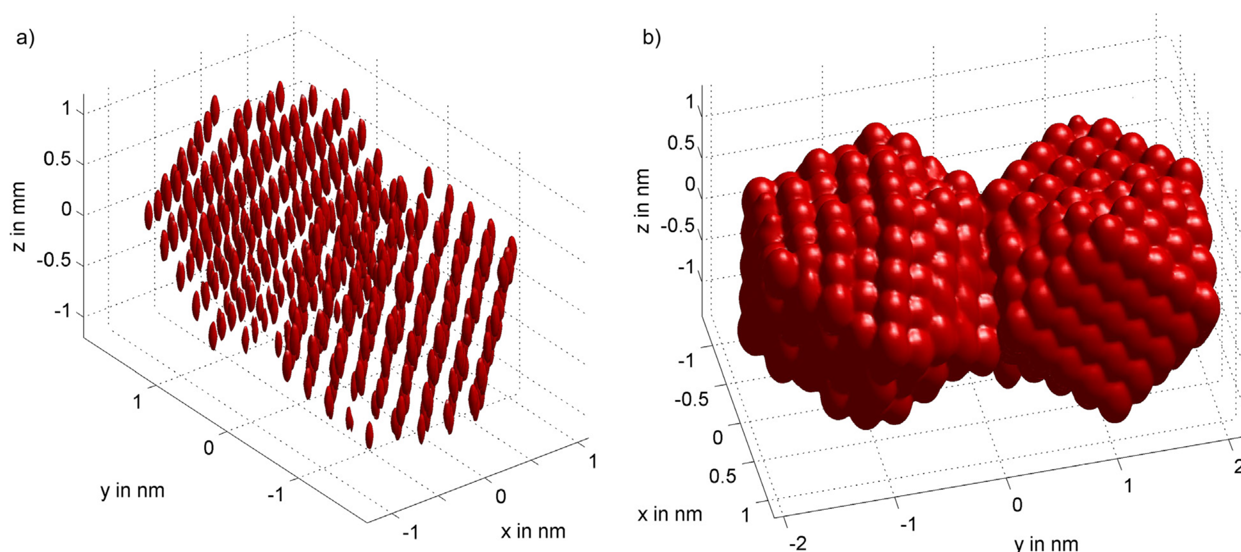

Fig. 3. (Color online.) 3D isosurface plots of the electrostatic potential reconstructed from a tilt series of HRTEM images. Two different isosurfaces of the model in two different orientations are shown in order to reveal the 3D positions of individual atoms (a) and also the different facets of the nanocrystals (b).

quite sparse indeed. CS theory now allows us to reconstruct a three-dimensional object potential which is compatible with the measurements (whether they be HRTEM images or diffraction patterns) and is maximally sparse, by demanding that the reconstruction has minimal ℓ_1-norm.

The amount of data that must be collected for achieving a unique reconstruction depends strongly on the degree of incoherence of the measurement with the object basis and, of course, on the amount of noise in the data. Under ideal conditions, the number of necessary measurements is proportional to the number of non-zero elements in the reconstructed object [51]. As illustrated above, a $5 \times 5 \times 5\ \text{nm}^3$ cube of silicon contains 6250 atoms. If the three-dimensional space of the object is sampled with discrete voxels, the number of non-zero voxels is of the order of 6250.[2] If, for the moment, we assume that we need $m = 10$ measurements per non-zero element (some CS-literature mentions proportionality factors of $m = 4$ [51] or even less), then we should be able to recover each atom from 62500 *independent* measurements. This is a surprisingly low number, since in the CS-framework each pixel of an image is considered a measurement, just one $5 \times 5\ \text{nm}^2$ image sampled on a $0.2 \times 0.2\ \text{Å}^2$ grid would suffice. The pixels in an image, however, are generally not independent: For instance, neighboring pixels tend to have similar gray values and are therefore positively correlated. Fortunately, the benefits of CS appear to hold up in many practical situations as well: in [52], an exact tomographic reconstruction of the Shepp–Logan phantom from a very limited number of projections is achieved; in [53,54], the benefits of CS over conventional tomography are illustrated with many experimental reconstructions of materials science systems; and in [17] CS achieves atomic-scale determination of the surface facets of Au-nanorods from a limited number of projections. However, due to the requirement of the validity of the projection requirement, i.e. the contribution of a whole column of voxels to only a single pixel in a given projection, the coherence between measurement and object basis in linear tomography is quite high. Multiple scattering and delocalization as encountered in HRTEM imaging with low-energy electrons must cause a higher degree of incoherence between measurement and object basis and thus even more may be gained from the application of CS principles.

The example in Fig. 2a shows a model of two gold cuboctahedron-shaped nanoparticles, each one containing 309 atoms. Due to the orientation of the left particle in the (311) zone axis, the atoms appear very closely spaced. Fig. 2b shows example HRTEM images simulated for different tilt angles of this model under parallel illumination. The range of tilt angles ($\pm 10^\circ$) is very small compared to what would be required for a linear tomography reconstruction. However, although the very small projected interatomic distances in the (311)-oriented particle cannot be resolved in any of these images, multiple scattering of the 40-keV electrons encodes the three-dimensional positions of all the atoms in the images.

Applying our recently developed algorithm for the inversion of dynamical electron scattering (IDES) to the HRTEM images, examples of which are shown in Fig. 2b, the three-dimensional object potential can be reconstructed. Fig. 3 shows two different isosurface renderings. In Fig. 3a, the positions of all the atoms in the two particles are revealed, while in Fig. 3b the different facets of the cuboctahedra are emphasized.

While Fig. 3 may give some impression of the quality of the reconstruction, displaying the individual potential layers used to simulate the HRTEM images and their counterparts from the reconstructed volume (Fig. 4) facilitates a more quantitative

[2] Following the approach in [45] of writing the object as a convolution of an array of Dirac delta-functions centered on the atom positions with the known atomic potential of Si yields a number of non-zero elements exactly equal to the number of atoms, i.e. 6250.

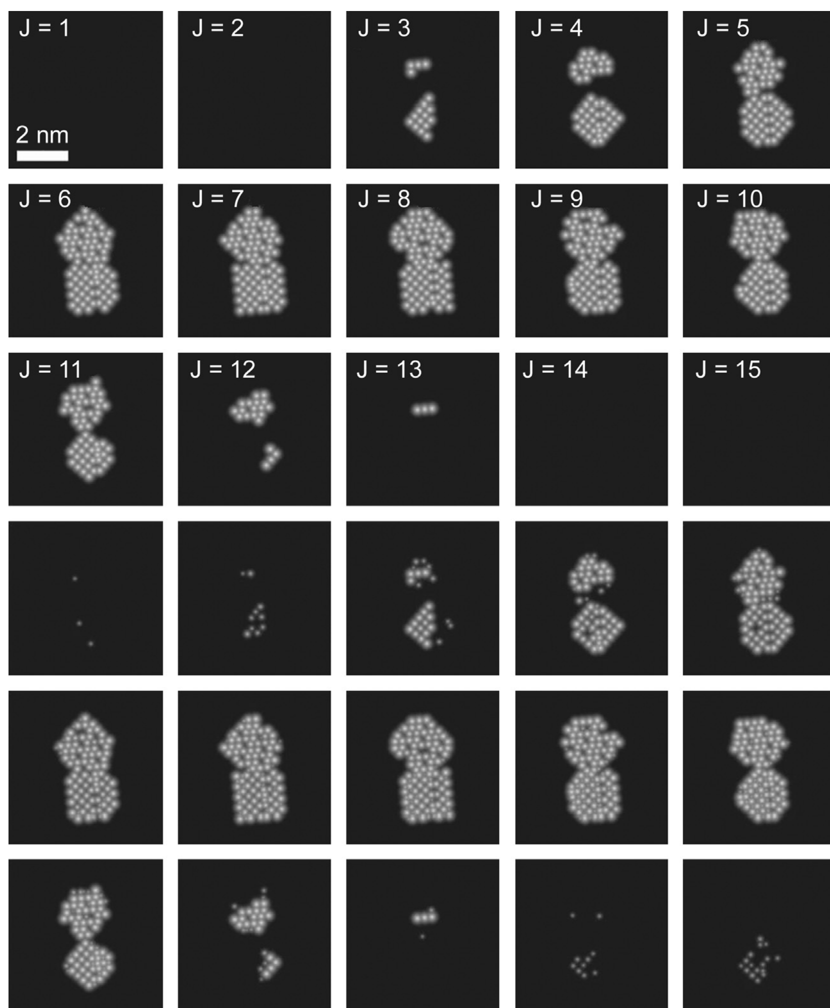

Fig. 4. Layers of the original (top three rows) and IDES-reconstructed (bottom three rows) electrostatic potential, displayed on a logarithmic scale. Both, input potential, and reconstructed potential were sliced into 15 slices.

comparison between input model and reconstruction. Although both inelastic and elastic scattering potential have been reconstructed, only the elastic scattering potential is shown. Comparing the potential slices in the top three rows with the corresponding slices comprising the reconstructed potential, all the atoms are present, and a few small additional peaks (enhanced by the logarithmic scale of the images) appear. These additional peaks are mostly vertical extensions of atoms in layers above or below, reflecting the finite z-resolution of the reconstruction due to the very small tilt range used in these simulations. However, at about 2 Å the z-resolution is on par with the point resolution of 1.5 Å, which is quite remarkable considering the tilt range of only $\pm 10^\circ$.

4. Conclusion

We have shown that accurate dose-efficient measurement of the three-dimensional positions of atoms in thin samples is indeed possible. These measurements are possible by combining the principle of compressed sensing and a numerical algorithm inverting the multislice algorithm commonly used for multiple scattering simulations in TEM image simulations. This combination harnesses the 3D information encoded in interference patterns produced by multiply scattered electrons and may achieve very high resolution along the z-direction from HRTEM or diffraction data acquired for a small range of specimen (or beam-) tilt angles. This makes it possible to obtain 3D atomic resolution also for conventional, planar specimen geometries which cause self-shadowing at high specimen tilts required for conventional tomography. The fact that multiple elastic scattering is fully accounted for makes this technique applicable at low accelerating voltages. However, the theoretical framework is equally well applicable at higher accelerating voltages, but may require a slightly larger range of tilt angles in order to achieve equally high resolution along the direction parallel to the electron beam.

Acknowledgements

This work has been funded by the Carl Zeiss Foundation as well as the German Research Foundation (DFG, Grant No. KO 2911/7-1).

References

[1] R. Henderson, Q. Rev. Biophys. 28 (1995) 171–193.
[2] A.V. Crewe, J. Wall, J. Langmore, Science 168 (1970) 1338–1340.
[3] P.D. Nellist, S.J. Pennycook, Science 274 (1996) 413–415.
[4] P. Voyles, D.A. Muller, J.L. Grazul, P.H. Citrin, H.-J.L. Gossmann, Nature 416 (2002) 826–829.
[5] J.C. Meyer, S. Kurasch, H.J. Park, V. Skakalova, D. Künzel, A. Groß, A. Chuvilin, G. Algara-Siller, S. Roth, T. Iwasaki, U. Starke, J.H. Smet, U. Kaiser, Nat. Mater. 10 (2011) 209–215.
[6] W. Zhou, M.P. Oxley, A.R. Lupini, O.L. Krivanek, S.J. Pennycook, J.-C. Idrobo, Microsc. Microanal. 18 (2012) 1342–1354.
[7] M. Haider, H. Rose, S. Uhlemann, E. Schwan, B. Kabius, K. Urban, Ultramicroscopy 75 (1998) 53–60.
[8] O.L. Krivanek, N. Dellby, A.J. Spence, R.A. Camps, L.M. Brown, IOP Conf. Ser. 153 (1997) 35–40.
[9] C. Kisielowski, B. Freitag, M. Bischoff, H. van Lin, S. Lazar, G. Knippels, P. Tiemeijer, M. van der Stam, S. von Harrach, M. Stekelenburg, M. Haider, S. Uhlemann, H. Müller, P. Hartel, B. Kabius, D. Miller, I. Petrov, E.A. Olson, T. Donchev, E.A. Kenik, A.R. Lupini, J. Bentley, S.J. Pennycook, I.M. Anderson, A.M. Minor, A.K. Schmid, T. Duden, V. Radmilovic, Q.M. Ramasse, M. Watanabe, R. Erni, E.A. Stach, P. Denes, U. Dahmen, Microsc. Microanal. 14 (2008) 469–477.
[10] P.K. Luther, in: J. Frank (Ed.), Electron Tomography, Three-Dimensional Imaging with the Transmission Electron Microscope, Plenum Press, New York, 1992.
[11] T.F. Kelly, D.J. Larson, Annu. Rev. Mater. Res. 42 (2012) 1–31.
[12] S. Van Aert, A.J. Den Dekker, V.A. den Bos, D. van Dyck, Adv. Imaging Electron Phys. 130 (2004) 1–164.
[13] S. Van Aert, K.J. Batenburg, M.D. Rossell, R. Erni, G. Van Tendeloo, Nature 470 (2011) 374–377.
[14] P.D. Nellist, P. Wang, Annu. Rev. Mater. Res. 42 (2012) 125–143.
[15] K. van Benthem, A.R. Lupini, M. Kim, H. Suck Baik, S. Doh, J.-H. Lee, M.P. Oxley, S.D. Findley, L.J. Allen, J.T. Tuck, S.J. Pennycook, Appl. Phys. Lett. 87 (2005) 034104.
[16] W. Van den Broek, S. Van Aert, D. Van Dyck, Ultramicroscopy 110 (2010) 548–554.
[17] B. Goris, S. Bals, W. Van den Broek, E. Carbó-Argibay, S. Gomez-Grana, L.M. Liz-Marzan, G. Van Tendeloo, Nat. Mater. 11 (2012) 930–935.
[18] C.-C. Chen, C. Zhu, E.R. White, C.-Y. Chiu, M.C. Scott, B.C. Regan, L.D. Marks, Y. Huang, J. Miao, Nature 496 (2013) 74–79.
[19] W. Van den Broek, S. Van Aert, D. Van Dyck, Ultramicroscopy 109 (2009) 1485–1490.
[20] W. Van den Broek, A. Rosenauer, B. Goris, G. Martinez, S. Bals, S. Van Aert, D. Van Dyck, Ultramicroscopy 116 (2012) 8–12.
[21] G. Mollenstedt, H. Wahl, Naturwissenschaften 55 (1968) 340–341.
[22] H. Lichte, P. Formanek, A. Lenk, M. Linck, C. Matzeck, M. Lehmann, P. Simon, Annu. Rev. Mater. Res. 37 (2007) 539–588.
[23] E.J. Kirkland, Ultramicroscopy 15 (1984) 151–172.
[24] A.I. Kirkland, W.O. Saxton, K.L. Chau, K. Tsuno, M. Kawasaki, Ultramicroscopy 57 (1995) 355–374.
[25] W.M.J. Coene, A. Thust, M. Op de Beek, D. Van Dyck, Ultramicroscopy 64 (1996) 109–135.
[26] T. Kawasaki, Y. Takai, T. Ikuta, R. Shimizu, Ultramicroscopy 90 (2001) 47–59.
[27] L.J. Allen, M.P. Oxley, Opt. Commun. 199 (2001) 65–75.
[28] T. Kawasaki, Y. Takai, Surf. Interface Anal. 35 (2003) 51–54.
[29] W.-K. Hsieh, F.-R. Chen, J.-J. Kai, A.I. Kirkland, Ultramicroscopy 98 (2004) 99–114.
[30] L.J. Allen, W. McBride, N.L. O'Leary, M.P. Oxley, Ultramicroscopy 100 (2004) 91–104.
[31] C.T. Koch, Ultramicroscopy 108 (2008) 141–150.
[32] C.T. Koch, A. Lubk, Ultramicroscopy 110 (2010) 460–471.
[33] P. Thibault, V. Elser, Annu. Rev. Condens. Matter Phys. 1 (2010) 237–255.
[34] K.A. Nugent, Adv. Phys. 59 (2010) 1–99.
[35] W. Hoppe, Ultramicroscopy 10 (1982) 187–198.
[36] H.M.L. Faulkner, J.M. Rodenburg, Phys. Rev. Lett. 92 (2004) 023903.
[37] C.B. Boothroyd, R.E. Dunin-Borkowski, Ultramicroscopy 98 (2004) 115–133.
[38] D. Muller, B. Edwards, E. Kirkland, J. Silcox, Ultramicroscopy 86 (2001) 371–380.
[39] J.M. LeBeau, S.D. Findlay, L.J. Allen, S. Stemmer, Phys. Rev. Lett. 100 (2008) 206101.
[40] G. Möbus, T. Gemming, P. Gumbsch, Acta Crystallogr. A 54 (1998) 83–90.
[41] C.T. Koch, Determination of core structure and point defect density along dislocations, PhD thesis, Arizona State University, 2002.
[42] D. Van Dyck, J.R. Jinschek, F.-R. Chen, Nature 486 (2012) 243–246.
[43] A. Wang, S. Van Aert, P. Goos, D. Van Dyck, Ultramicroscopy 114 (2012) 20–30.
[44] G. Oszlanyi, A. Suto, Acta Crystallogr. A 60 (2004) 134–141.
[45] W. Van den Broek, C.T. Koch, Phys. Rev. Lett. 109 (2012) 245502.
[46] W. Van den Broek, C.T. Koch, Phys. Rev. B 87 (2013) 184108.
[47] W. Van den Broek, S. Van Aert, D. Van Dyck, Microsc. Microanal. 18 (2012) 336–342.
[48] J. Romberg, IEEE Signal Process. Mag. 25 (2008) 14–20.
[49] R. Baraniuk, IEEE Signal Process. Mag. 24 (2007) 118–121.
[50] E.J. Candés, J.K. Romberg, T. Tao, Commun. Pure Appl. Math. 59 (2006) 1207.
[51] E. Candes, J. Romberg, Inverse Probl. 23 (2007) 969–985.
[52] E. Candes, J. Romberg, T. Tao, IEEE Trans. Inf. Theory 52 (2006) 489–509.
[53] B. Goris, W. Van den Broek, K. Batenburg, H.H. Mezerji, S. Bals, Ultramicroscopy 113 (2012) 120–130.
[54] R. Leary, Z. Saghi, P.A. Midgley, D.J. Holland, Ultramicroscopy 131 (2013) 70–91.